Determining Orientations of Optical Transition Dipole Moments Using Ultrafast X-ray Scattering

Determining Orientations of Optical Transition Dipole Moments using Ultrafast X-Ray Scattering

Haiwang Yong,[1] Nikola Zotev,[2] Brian Stankus,[1] Jennifer M. Ruddock,[1] Darren Bellshaw,[2] Sébastien Boutet,[3] Thomas J. Lane,[3] Mengning Liang,[3] Sergio Carbajo,[3] Joseph S. Robinson,[3] Wenpeng Du,[1] Nathan Goff,[1] Yu Chang[1], Jason E. Koglin,[3] Max D.J. Waters,[4] Theis I. Sølling,[4,$] Michael P. Minitti,[3] Adam Kirrander,[2,*] and Peter M. Weber[1,*]

[1]*Brown University, Department of Chemistry, Providence, Rhode Island 02912, USA*
[2]*School of Chemistry, University of Edinburgh, Edinburgh EH9 3FJ, United Kingdom*
[3]*SLAC National Accelerator Laboratory, Menlo Park, California 94025, USA*
[4]*Department of Chemistry, University of Copenhagen, Universitetsparken 5, 2100 Copenhagen, Denmark.*

[$]*Present address: Center for Integrative Petroleum Research, College of Petroleum & Geosciences, King Fahd University of Petroleum & Minerals, Dhahran 31261, Saudi Arabia*

AUTHOR INFORMATION

Corresponding Author

*E-mail: peter_weber@brown.edu (P. M. W.); adam.kirrander@ed.ac.uk (A. K.)

ABSTRACT: The identification of the initially prepared, optically active state remains a challenging problem in many studies of ultrafast photoinduced processes. We show that the initially excited electronic state can be determined using the anisotropic component of ultrafast time-resolved X-ray scattering signals. The concept is demonstrated using the time-dependent X-ray scattering of N-methyl morpholine in the gas-phase upon excitation by a 200 nm linearly polarized optical pulse. Analysis of the angular dependence of the scattering signal near time zero renders the orientation of the transition dipole moment in the molecular frame and identifies the initially excited state as the $3p_z$ Rydberg state, thus bypassing the need for further experimental studies to determine the starting point of the photoinduced dynamics and clarifying inconsistent computational results.

TOC GRAPHICS

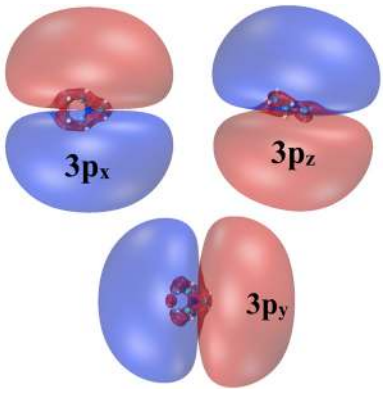

KEYWORDS. X-ray scattering, ultrafast dynamics, Rydberg states, molecular alignment, transition dipole moment, optical excitation.

The identification of the initially excited electronic state in ultrafast time-resolved experiments is of paramount importance for the analysis of the observed dynamics. Inaccurate assignment can lead to falsely attributed structural changes and to pathways that may not be accessible in the given experiments. Yet accurate assignments remain challenging, especially of the transient electronically excited states that constitute the critical initial step of any photochemical or photophysical process. We demonstrate here a method to assign the excited state via the orientation of the optical transition dipole moment (TDM) in the course of time-resolved, anisotropic x-ray scattering measurements.

Traditionally, TDMs are determined spectroscopically[1]. Experimental techniques such as 1D and 2D IR spectroscopy[2], fluorescence spectroscopy[3,4] and photoelectron spectroscopy[5,6] can be used for long-lived states. In addition, related properties such as oscillator strength and excitation energies are often obtained from electronic structure calculations and serve as supporting evidence for pinpointing the initially excited states. However, these strategies do not always provide unambiguous results. On the one hand, the experimental spectra may exhibit broadening that results from either instrumental parameters or the natural linewidth of the underlying transitions. If the molecular system features an ultrashort-lived state with a lifetime short compared to the rotational period, a molecular frame transition dipole moment can be determined from the photofragment angular distributions.[7–12] However, the determination of the TDM orientation in other cases remains intractable, while excitation energies, TDMs and oscillator strengths derived from computations are often associated with large uncertainties,[13,14] not the least in molecules where the initially excited state has Rydberg character and thus highly diffuse orbitals.[15,16] The identification of the initially excited state is therefore a challenging problem.

In this Letter we illustrate how the aforementioned complications can largely be bypassed in gas-phase ultrafast time-resolved X-ray scattering experiments, which have become possible with the recent development of powerful X-ray Free-Electron Lasers (XFELs). Within a few years of the first X-rays emerging from the Linac Coherent Light Source (LCLS),[17] ultrafast gas phase X-ray scattering experiments have become a reality, yielding scattering data with high temporal and angular resolution.[18–20] It is now feasible to obtain high-quality two-dimensional scattering signals that reveal the alignment and anisotropy in the sample.[21] Thus, in addition to the isotropic signal that reveals the structural dynamics, one can also explore the richness of information hidden in the anisotropy of the time-resolved X-ray scattering patterns. The potential importance of the anisotropic components of X-ray and electron scattering in gas-phase ensembles, and the accompanying rotational dynamics, is underscored by the fact that they have been studied theoretically for many years.[22–28] Experimental studies of rotational and structural dynamics of gas-phase molecules have also been performed by Yang *et al*. using time-resolved ultrafast electron diffraction.[29–33] In the present study, we show that for short lived states in polyatomic molecules, for which TDM orientations are difficult to obtain, the anisotropic scattering signal reveals the identity of the initially prepared state. We investigate the optical excitation of an asymmetric top molecule, N-methyl Morpholine (NMM) shown in Figure 1, using a 200 nm pump laser pulse in the gas phase and show that the anisotropy near time zero can be used as a quick and reliable tool to determine the initially accessed state.

The time-resolved molecular dynamics of NMM has previously been explored using Rydberg Fingerprint Spectroscopy.[34,35] Zhang *et al*. found that optical excitation at 208 nm prepares the molecule in a 3p state , which then decays via an internal conversion on a time scale of about 100 fs to the lower-lying 3s Rydberg state.[35] In the spectrum, they noticed that the 3p peak right after

time zero splits into two components, one intense peak with higher binding energy (BE) and one weaker peak at lower BE. Based on the relative order of binding energies calculated from self-interaction corrected density functional theory (DFT-SIC), the high BE and the low BE peaks were assigned to the $3p_z$ and $3p_x$ states, respectively. However, this identification of the initially excited state is only as reliable as the supporting computational results. To examine this last point, we show in Table 1 the computational results for the 3p Rydberg states of NMM at three different levels of theory. While the benchmark multireference configuration interaction (MRCI) and complete active space self-consistent field (CASSCF) methods indicate that the most probable excitation is to the $3p_z$ state, the time-dependent density functional theory (TDDFT) suggests that it is a $3p_y$ state. It is also worth noting that MRCI and CASSCF calculations suggest that vertical excitations energies are ordered as $3p_z<3p_x<3p_y$, but for TDDFT the order is $3p_x<3p_y<3p_z$. (See details in SI) Because of the inconsistencies in the computational results for challenging cases such as Rydberg-excited molecules, an unambiguous determination of short-lived optically excited states provides a valuable experimental benchmark.

Table 1. Oscillator strengths with TDM directions, shown as (x,y,z) unit vectors, from the ground state to each of the three 3p states in NMM, calculated at different levels of theory. Molecular axes are defined by the three principal rotational axes of NMM (Figure 1).

Excited State	CAM-B3LYP/6-311++G(d,p)	SA5-CASSCF(2,5)/6-311+G(d)	MRCI(2,5)/6-311+G(d)
$3p_x$	0.0041 (1, 0, 0)	0.0704 (1, 0, 0)	0.0322 (1, 0, 0)
$3p_y$	0.1159 (0, 0.57, -0.82)	0.0496 (0, 0.84, 0.55)	0.0340 (0, 0.85, 0.52)
$3p_z$	0.0318 (0, 0.15, 0.99)	0.1321 (0, 0.18, -0.98)	0.1138 (0, 0.18, -0.98)

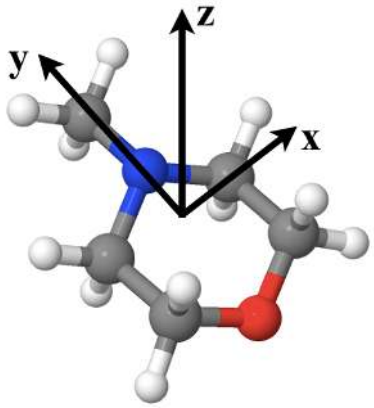

Figure 1. Structure and molecular axes of NMM in the ground state.

In the time-resolved x-ray scattering experiments, a thermal ensemble of room temperature gas-phase NMM molecules is excited with a 200 nm pump laser and probed using 9.5 keV x-ray photons generated by the Linac Coherent Light Source (LCLS). The scattering signal is detected on a 2.3-megapixel Cornell-SLAC Pixel Array Detector (CSPAD)[36] and the position of the detected x-rays is converted into the polar coordinates on the detector, expressed in terms of the amplitude of the scattering vector q and the azimuthal angle ϕ. The optical laser and the x-rays propagate collinearly, and their linear polarizations are perpendicular to each other. The time-evolving patterns are expressed as the percent difference scattering patterns, $P_{diff}(\phi, q, t)$,

$$P_{diff}(\phi, q, t) = 100 \frac{I_{on}(\phi,q,t) - I_{off}(\phi,q)}{I_{off}(\phi,q)}, \quad (1)$$

where $I_{on}(\phi, q, t)$ represents the scattering pattern at a given pump-probe delay time t, and $I_{off}(\phi, q)$ is the scattering pattern from the ground state, un-excited molecules, with ϕ the azimuthal angle on the detector and q the momentum transfer. Using the percent difference of the scattering signal helps to cancel poorly defined experimental parameters such as background signals and gas pressure fluctuations. More importantly, the anisotropy due to the polarization of

the X-rays also cancels out in Equation 1,[37] leaving only the anisotropy introduced by the optical pump pulse. The percent difference signal scales with the excitation probability, which is intentionally kept small as to reduce the probability of competing multi-photon excitation processes. Details about the experiments are described in the Supporting Information.

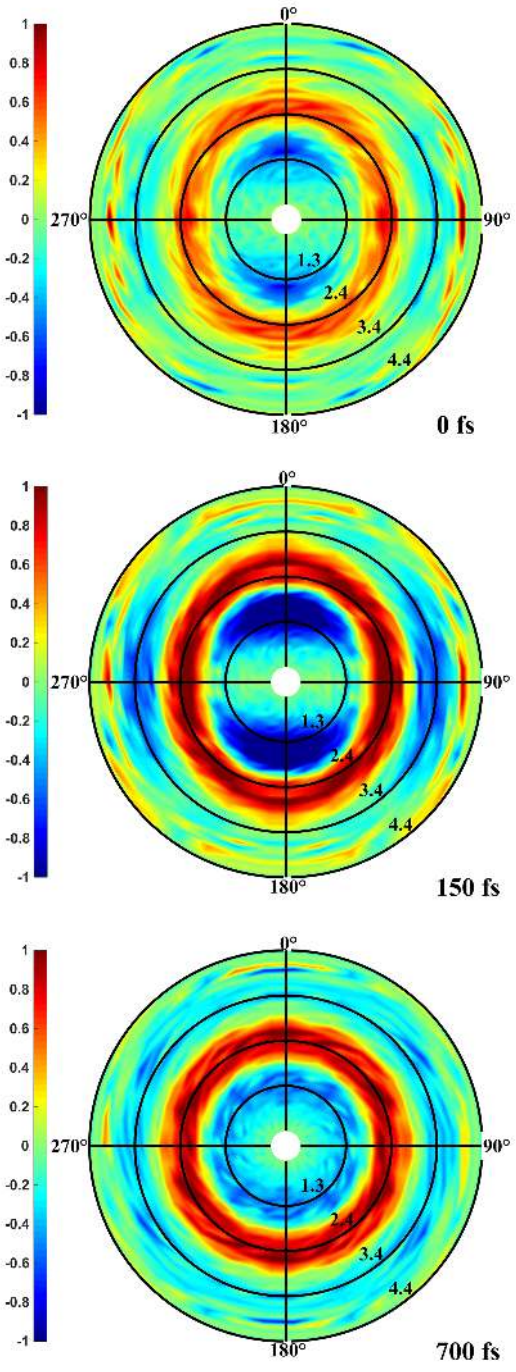

Figure 2. Experimental percent difference scattering patterns at three pump-probe delay times (0 fs, 150 fs, and 700 fs). The vertical axis is defined by the orientation of the polarization axis of the pump laser. The circles in the panels indicate values of the amplitude of the scattering momentum transfer vector of q =1.3, 2.4, 3.4, and 4.4 $Å^{-1}$.

The time-dependent scattering images shown in Figure 2 display a strong anisotropy near time zero, which decays at later times. The isotropic, radial dependence of the percent difference signal encodes the NMM dynamics as the molecule evolves from the ground state structure to the Rydberg state geometry after the optical excitation. The variation of the scattering signal with the azimuthal angle, i.e. the anisotropy, originates from the preferential excitation of those molecules whose TDM vector aligns with the polarization of the optical pulse in the laboratory frame. For a single-photon excitation the anisotropy takes a $\cos^2(\theta)$ functional form with respect to the laser polarization axis, where θ is defined as the angle between the molecular TDM vector and the laser polarization vector and ranges from 0 to π.[38] It follows that the intrinsic orientation of the TDM in the molecular frame determines the orientation of the excited state population of molecules in the laboratory frame, which is captured in the scattering signal near time zero. Since the alignment of excited molecules is determined by the relationship between the TDM vector of the initially accessed state and the laser polarization vector, the ultrashort lifetime of the initially excited states, or any subsequent dynamics, will not destroy the $\cos^2(\theta)$ distribution imparted on the ensemble with the excitation. For symmetric and asymmetric tops and linear molecules, different orientations of the TDM vectors in the molecular frame produce markedly different scattering signals regardless of their relative magnitude. Since their orientation is often constrained by the point group of the molecule, straightforward scattering pattern symmetry arguments possibly assisted by structures derived from inexpensive calculations can be used to unambiguously determine the initially excited state.

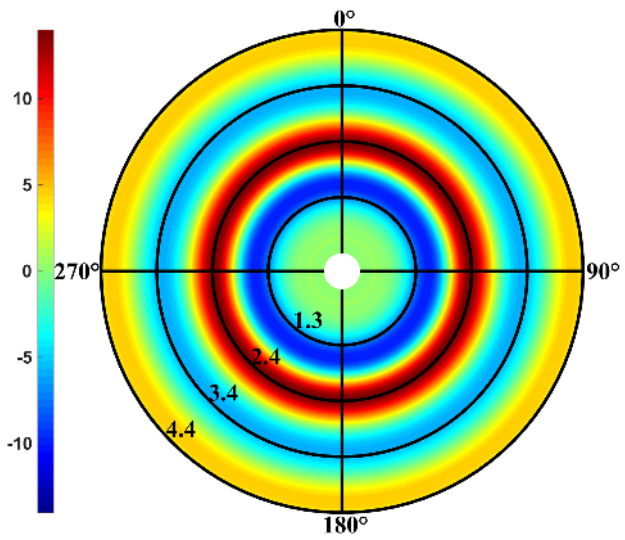

Figure 3. Simulated percent difference scattering pattern produced using the rotationally averaged independent atom model (IAM)[39] showing the isotropic result once the alignment disappears (100% excitation is assumed). The excited state molecular geometry used corresponds to the optimized geometry of the molecular ion, which is also used in modeling the I_{on} signal in Figure 4.

It is worth pointing out that ultrafast X-ray scattering experiments ultimately measure geometry changes. Although the maximum molecular alignment occurs at time zero, the maximum strength of the anisotropy is observed only when the geometry has evolved significantly. In other words, even though the excited molecules are preferentially aligned with the laser polarization axis, without a significant geometry change, the populations of the ground and the excited states are indistinguishable by X-ray scattering. It is worth noting that the detection of the instantaneous rearrangement of the electrons after a photon absorption, which is a much weaker effect, remains elusive. As the geometry evolves, the rotational wavepackets formed on the excited and the ground states disperse, resulting in a loss of alignment. These two effects, i.e. rotational and internal motion, compete, which results in the anisotropic scattering having maximum magnitude at 150 fs in the case of NMM. In general, because rotational motion

is much slower than the molecular frame structural dynamics, the anisotropy should be detectable in a majority of molecular systems. In NMM, as is evident from the data, rotational dephasing fully destroys the $\cos^2(\theta)$ alignment in approximately 700 fs, while a near-equilibrium geometry for the Rydberg state is reached in less than 250 fs. Subsequent vibrational motion and subtle geometry transformations shift the peak positions in the q-dependent signal without affecting significantly the overall shape and orientation of the observed anisotropy. This makes the anisotropy near time zero a simple but powerful tool for determining the initially excited state prior to any detailed analysis of the underlying dynamics.

The quadrant symmetry of the observed signal is explained by the orientational freedom around the polarization axis. Close inspection of the anisotropy in the images in Figure 2 reveals that the angular dependence peaks near q=1.3 $Å^{-1}$ and q=3.4 $Å^{-1}$. The amplitude of the negative peak at q=1.3 $Å^{-1}$ is at a maximum in vertical direction, while the negative signal near q=3.4 $Å^{-1}$ is stronger in the horizontal direction. The positive feature at q=2.4 $Å^{-1}$ does not show a strong anisotropy, besides a slight stretch along the vertical axis.

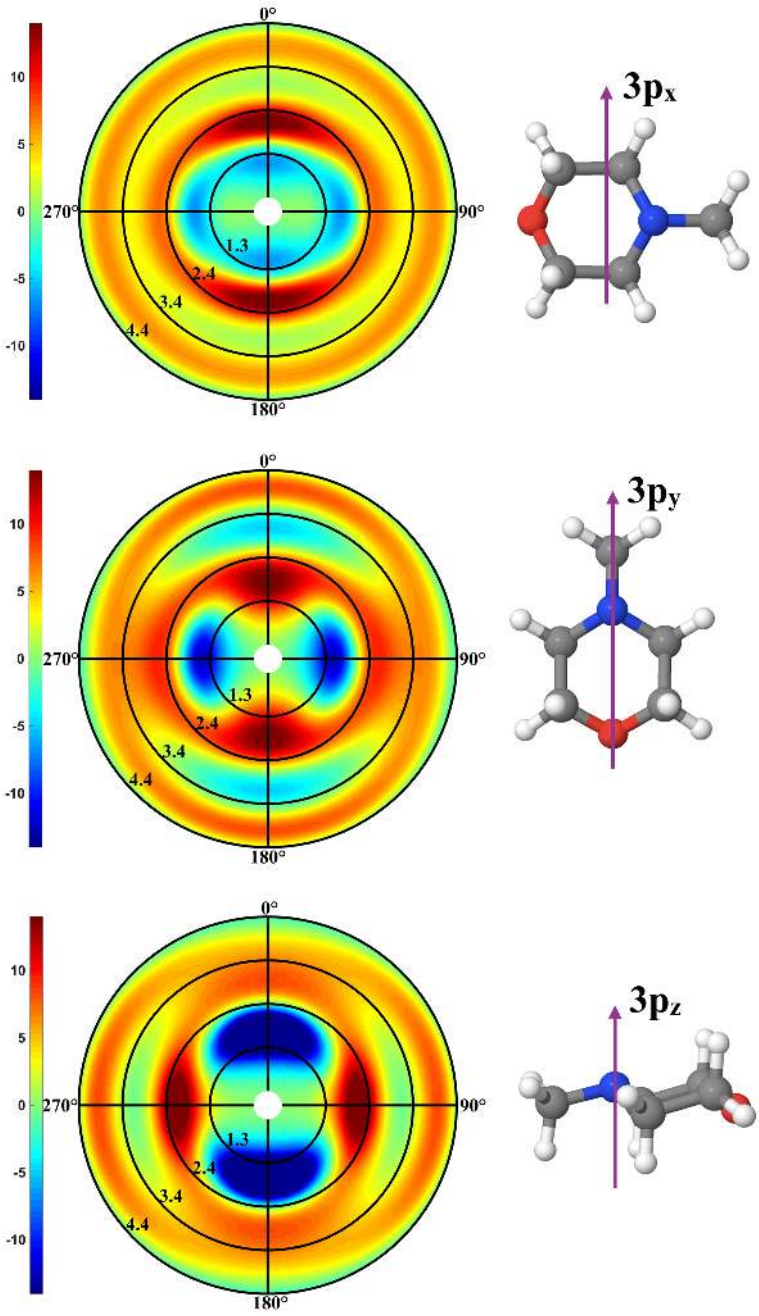

Figure 4. Simulated percent difference scattering patterns for NMM molecules, left column, excited to the $3p_x$, $3p_y$ and the $3p_z$ electronic Rydberg states, with the orientation of the transition dipole moment relative the molecule shown in the right column. A $\cos^2(\theta)$ distribution with respect to the laser polarization axis is assumed and orientations due to rotation about the laser polarization axis are averaged out. In the right column the orientation of the TDM in the molecular frame is indicated using a purple arrow, as calculated from MRCI(2,5)/6-311+G(d).

For the purpose of calculating reference scattering intensities, the optimized geometry of the ion-state NMM from UMP2/aug-cc-pVDZ is used to approximate the Rydberg state structure. While not strictly accurate, the resulting error in the isotropic signal has only a small effect on the anisotropic component of the signal. The isotropic difference signal is calculated as shown in Figure 3, which agrees favorably with the experimental pattern following rotational dephasing (at approximately t>700 fs). In order to identify the initially excited state, we create a $\cos^2(\theta)$ distribution of excited molecules in an ensemble for the three possible cases of alignment, corresponding to the polarization axis being aligned with the TDM axis of the $3p_x$, the $3p_y$ or the $3p_z$ state. The calculated percent difference scattering patterns are presented in Figure 4. It is apparent that only the simulated pattern of the $3p_z$ excitation shows the same symmetry as the experiment (see Figure 2, 0 fs and 150 fs panel). However, because the assumption of an instantaneous geometry change is made in the simulations of the results in Figure 4, and because the percent difference signals can be detected only when there is a difference in structures between the unexcited and the excited molecules, the angular distribution seen in the anisotropic scattering pattern can never be measured exactly as shown in Figure 4 (note the discrepancy in the angular distributions near q=2.4 $Å^{-1}$ for $3p_z$ as compared to Figure 2). The experimental measurement, Figure 2, shows the pattern on the path from the anisotropic signal approximated as a $\cos^2(\theta)$ distribution to the isotropic signal when the alignment is completely lost to rotational motion.

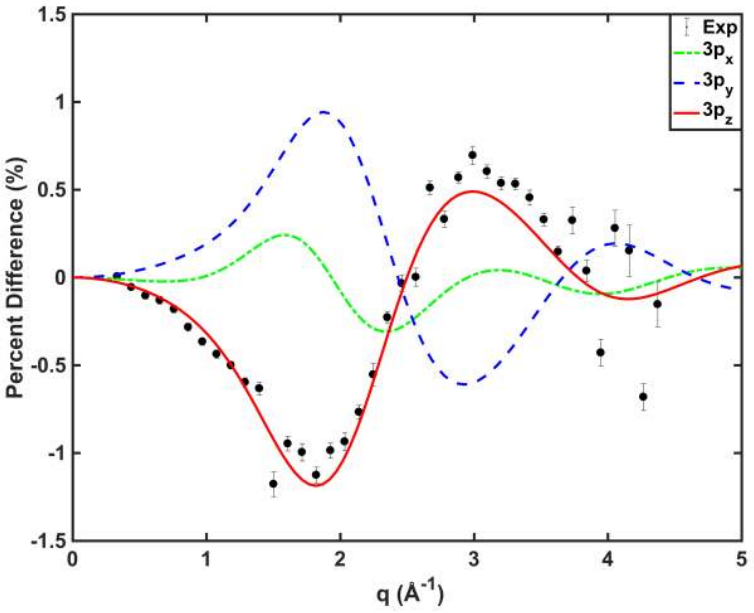

Figure 5. The anisotropic signal derived from experimental results at a pump-probe delay time of t=150 fs. The three theoretical signals are derived from the calculated results shown in Figure 4. The theoretical curves are scaled with respect to the excitation fraction, and dephasing of the $\cos^2(\theta)$ distribution after time zero is taken into consideration.

In order to quantify the difference between the three states of interest, the amplitude of their anisotropic scattering components, which reflect the angular distributions of the total signal, are decomposed from the 2-dimensional scattering pattern using a standard method (see details in SI),[24,26–28] and compared to the anisotropic component of experimental result at 150 fs, which shows maximum anisotropy. (The results using other times are shown in the SI.) As is evident from Figure 5, the anisotropic signal derived from the experimental scattering pattern only matches that of the $3p_z$ Rydberg state, for which the TDM points along the lone pair of the nitrogen atom. The three calculated signals are remarkably different on account of the orthogonality of their TDMs, which makes identification of the state straightforward. Specifically, the $3p_z$ and $3p_y$ anisotropy components are nearly opposite of each other, while the

$3p_x$ anisotropy components have different peak centers and much smaller magnitudes compared to $3p_y$.

It is possible to imagine situations where a wavepacket is launched on several electronic states, in which case the anisotropy will have contributions from all states involved. Under these circumstances, depending on the relative orientations of their TDMs, it might be possible to apply a fitting procedure to determine even the relative excitation fractions of these states. In the case of NMM, this is not necessary as the experimental results are clearly explained by the $3p_z$ state alone. This is to be expected given the bandwidth of the pump laser, which is around 1 nm (full width at half maximum), the large energy differences of the 3p states,[35] and the difference in the oscillator strengths from the benchmark MRCI(2,5)/6-311+G(d) calculation in Table 1.

The current experiment also yields time-dependent scattering signals of the coherent vibrational motion in NMM on the 3s potential energy surface following $3p_z \rightarrow 3s$ internal conversion. The full analysis of this motion requires in-depth calculations of the electron density distributions and quantum molecular dynamics that account for the vibrational dephasing of the coherent vibrations and the nonadiabatic coupling between electronic and nuclear motions. Such an analysis of the presented data is currently underway with the aim of a complete understanding of the photoexcited dynamics and will be reported later.

In contrast to other pump-probe techniques, where the determination of the initially excited state is limited by the availability of complementary spectra or the accuracy of the computed oscillator strengths, ultrafast X-ray scattering experiments provides inherent information for the electronic transition induced by the pump pulse. In this Letter, we demonstrate how the strong anisotropy detected immediately after photoexcitation leads to fast and reliable identification of the initially excited state relying only on the orientation of the TDM in the molecular frame.

Because the alignment of the molecules in the ensemble is preserved for a long time compared to the lifetime of the excited state, this method is applicable despite the fast internal conversion after excitation. Ultimately, the advantage of X-ray scattering stems from the fact that, unlike spectroscopy which deals with the energy levels, the scattering signal constitutes a direct observation of the molecular structure in space.

ASSOCIATED CONTENT

Supporting Information.

The following files are available free of charge on the ACS Publications website at DOI:xxx.

Experimental methods, computational details, anisotropy scattering separation and fitting. (PDF)

AUTHOR INFORMATION

Notes

The authors declare no competing financial interests.

ACKNOWLEDGMENT

Portions of this research were carried out on the CXI Instrument at the Linac Coherent Light Source (LCLS), a division of SLAC National Accelerator Laboratory and an Office of Science user facility operated by Stanford University. This work was supported by the U.S. Department of Energy, Office of Science, Basic Energy Sciences, under Award DE-SC0017995.

H.Y. and N.Z. contributed equally to this work.

REFERENCES

(1) Nordén, B. Applications of Linear Dichroism Spectroscopy. *Appl. Spectrosc. Rev.* **1978**, *14*, 157–248.

(2) Grechko, M.; Zanni, M. T. Quantification of Transition Dipole Strengths Using 1D and 2D Spectroscopy for the Identification of Molecular Structures via Exciton Delocalization: Application to α-Helices. *J. Chem. Phys.* **2012**, *137*, 184202.

(3) Zare, R. N.; Herschbach, D. R. Doppler Line Shape of Atomic Fluorescence Excited by Molecular Photodissociation. *Proc. IEEE* **1963**, *51*, 173–182.

(4) Mu, T.; Chen, S.; Zhang, Y.; Guo, P.; Chen, H. Determining the Orientation of Transition Moments and Depolarization by Fluorescence Polarizing Angle Spectrum. *Opt. Express* **2015**, *23*, 11748-11754.

(5) Lohmüller, T.; Erdmann, M.; Rubner, O.; Engel, V. Determination of Transition Dipole Moments from Time-Resolved Photoelectron Spectroscopy. *Eur. Phys. J. D* **2003**, *25*, 95–99.

(6) Reid, K. L. Photoelectron Angular Distributions. *Annu. Rev. Phys. Chem.* **2003**, *54*, 397–424.

(7) Dzvonik, M.; Yang, S.; Bersohn, R. Photodissociation of Molecular Beams of Aryl Halides. *J. Chem. Phys.* **1974**, *61*, 4408–4421.

(8) Kawasaki, M.; Lee, S. J.; Bersohn, R. Photodissociation of Molecular Beams of Aryl Halides: Translational Energy Distribution of the Fragments. *J. Chem. Phys.* **1977**, *66*, 2647–2655.

(9) Heck, A. J. R.; Chandler, D. W. Imaging Techniques for the Study of Chemical Reaction Dynamics. *Annu. Rev. Phys. Chem.* **1995**, *46*, 335–372.

(10) Fuglesang, C. D.; Baugh, D. A.; Pipes, L. C. Extraction of the Transition Dipole Matrix from the Photodissociation of Oriented/Aligned Parent Molecules. *J. Chem. Phys.* **1996**, *105*, 9796-9803.

(11) Sato, H. Photodissociation of Simple Molecules in the Gas Phase. *Chem. Rev.*, **2001**, *101*, 2687-2726.

(12) Rakitzis, T. P.; van den Brom, A. J.; Janssen, M. H. M. Directional Dynamics in the Photodissociation of Oriented Molecules. *Science* **2004**, *303*, 1852–1854.

(13) Dreuw, A.; Head-Gordon, M. Failure of Time-Dependent Density Functional Theory for Long-Range Charge-Transfer Excited States: The Zincbacteriochlorin-Bacteriochlorin and Bacteriochlorophyll-Spheroidene Complexes. *J. Am. Chem. Soc.* **2004**, *126*, 4007–4016.

(14) Prlj, A.; Curchod, B. F. E.; Fabrizio, A.; Floryan, L.; Corminboeuf, C. Qualitatively Incorrect Features in the TDDFT Spectrum of Thiophene-Based Compounds. *J. Phys. Chem. Lett.* **2015**, *6*, 13–21.

(15) Gudmundsdóttir, H.; Zhang, Y.; Weber, P. M.; Jónsson, H. Self-Interaction Corrected Density Functional Calculations of Molecular Rydberg States. *J. Chem. Phys.* **2013**, *139*, 194102.

(16) Cheng, X.; Zhang, Y.; Jónsson, E.; Jónsson, H.; Weber, P. M. Charge Localization in a Diamine Cation Provides a Test of Energy Functionals and Self-Interaction Correction. *Nat. Commun.* **2016**, *7*, 11013.

(17) Emma, P.; Akre, R.; Arthur, J.; Bionta, R.; Bostedt, C.; Bozek, J.; Brachmann, A.; Bucksbaum, P.; Coffee, R.; Decker, F. J.; et al. First Lasing and Operation of an Ångstrom-Wavelength Free-Electron Laser. *Nat. Photonics* **2010**, *4*, 641–647.

(18) Minitti, M. P.; Budarz, J. M.; Kirrander, A.; Robinson, J.; Lane, T. J.; Ratner, D.; Saita,

K.; Northey, T.; Stankus, B.; Cofer-Shabica, V.; et al. Toward Structural Femtosecond Chemical Dynamics: Imaging Chemistry in Space and Time. *Faraday Discuss.* **2014**, *171*, 81–91.

(19) Minitti, M. P.; Budarz, J. M.; Kirrander, A.; Robinson, J. S.; Ratner, D.; Lane, T. J.; Zhu, D.; Glownia, J. M.; Kozina, M.; Lemke, H. T.; et al. Imaging Molecular Motion: Femtosecond X-Ray Scattering of an Electrocyclic Chemical Reaction. *Phys. Rev. Lett.* **2015**, *114*, 255501.

(20) Glownia, J. M.; Natan, A.; Cryan, J. P.; Hartsock, R.; Kozina, M.; Minitti, M. P.; Nelson, S.; Robinson, J.; Sato, T.; van Driel, T.; et al. Self-Referenced Coherent Diffraction X-Ray Movie of Ångström- and Femtosecond-Scale Atomic Motion. *Phys. Rev. Lett.* **2016**, *117*, 153003.

(21) Küpper, J.; Stern, S.; Holmegaard, L.; Filsinger, F.; Rouzée, A.; Rudenko, A.; Johnsson, P.; Martin, A. V.; Adolph, M.; Aquila, A.; et al. X-Ray Diffraction from Isolated and Strongly Aligned Gas-Phase Molecules with a Free-Electron Laser. *Phys. Rev. Lett.* **2014**, *112*, 083002.

(22) Williamson, J. C.; Zewail, A. H. Ultrafast Electron Diffraction. 4. Molecular Structures and Coherent Dynamics. *J. Phys. Chem.* **1994**, *98*, 2766–2781.

(23) Ben-Nun, M.; Cao, J.; Wilson, K. R. Ultrafast X-Ray and Electron Diffraction: Theoretical Considerations. *J. Phys. Chem. A* **1997**, *101*, 8743–8761.

(24) Cao, J.; Wilson, K. R. Ultrafast X-Ray Diffraction Theory. *J. Phys. Chem. A* **1998**, *102*, 9523–9530.

(25) Baskin, J. S.; Zewail, A. H. Molecular Structure and Orientation: Concepts from Femtosecond Dynamics. *J. Phys. Chem. A* **2001**, *105*, 3680–3692.

(26) Baskin, J. S.; Zewail, A. H. Ultrafast Electron Diffraction: Oriented Molecular Structures in Space and Time. *ChemPhysChem* **2005**, *6*, 2261–2276.

(27) Baskin, J. S.; Zewail, A. H. Oriented Ensembles in Ultrafast Electron Diffraction. *ChemPhysChem* **2006**, *7*, 1562–1574.

(28) Lorenz, U.; Møller, K. B.; Henriksen, N. E. On the Interpretation of Time-Resolved Anisotropic Diffraction Patterns. *New J. Phys.* **2010**, *12*, 113022.

(29) Reckenthaeler, P.; Centurion, M.; Fuß, W.; Trushin, S. A.; Krausz, F.; Fill, E. E. Time-Resolved Electron Diffraction from Selectively Aligned Molecules. *Phys. Rev. Lett.* **2009**, *102*, 213001.

(30) Yang, J.; Makhija, V.; Kumarappan, V.; Centurion, M. Reconstruction of Three-Dimensional Molecular Structure from Diffraction of Laser-Aligned Molecules. *Struct. Dyn.* **2014**, *1*, 044101.

(31) Yang, J.; Centurion, M. Gas-Phase Electron Diffraction from Laser-Aligned Molecules. *Struct. Chem*. **2015**, *26*, 1513–1520.

(32) Yang, J.; Beck, J.; Uiterwaal, C. J.; Centurion, M. Imaging of Alignment and Structural Changes of Carbon Disulfide Molecules Using Ultrafast Electron Diffraction. *Nat. Commun.* **2015**, *6*, 8172.

(33) Yang, J.; Guehr, M.; Vecchione, T.; Robinson, M. S.; Li, R.; Hartmann, N.; Shen, X.; Coffee, R.; Corbett, J.; Fry, A.; et al. Diffractive Imaging of a Rotational Wavepacket in Nitrogen Molecules with Femtosecond Megaelectronvolt Electron Pulses. *Nat. Commun.* **2016**, *7*, 11232.

(34) Zhang, Y.; Deb, S.; Jónsson, H.; Weber, P. M. Observation of Structural Wavepacket Motion: The Umbrella Mode in Rydberg-Excited N-Methyl Morpholine. *J. Phys. Chem.*

Lett. **2017**, *8*, 3740–3744.

(35) Zhang, Y.; Jónsson, H.; Weber, P. M. Coherence in Nonradiative Transitions: Internal Conversion in Rydberg-Excited N-Methyl and N-Ethyl Morpholine. *Phys. Chem. Chem. Phys.* **2017**, *19*, 26403–26411.

(36) Blaj, G.; Caragiulo, P.; Carini, G.; Carron, S.; Dragone, A.; Freytag, D.; Haller, G.; Hart, P.; Hasi, J.; Herbst, R.; et al. X-Ray Detectors at the Linac Coherent Light Source. *J. Synchrotron Rad.* **2015**, *22*, 577–583.

(37) Als-Nielsen, J.; McMorrow, D. *Elements of Modern X-Ray Physics*, 2nd ed.; Wiley, **2011**.

(38) Zare, R. N. Optical Preparation of Aligned Reagents. *Ber. Bunsenges. Phys. Chem.* **1982**, *86*, 422–425.

(39) Prince, E. *International Tables for Crystallography. Volume C: Mathematical, Physical and Chemical Tables*, 3rd ed.; Springer, Dordrecht, **2006**.